

# Status of the ATLAS Experiment

*Kerstin Jon-And*<sup>1</sup>

*On behalf of the ATLAS Collaboration*

<sup>1</sup>Stockholm University, The Oskar Klein Centre for Cosmoparticle Physics, Department of Physics, AlbaNova, SE-106 91 Stockholm, Sweden

The ATLAS detector, which has been under construction and installation for close to 20 years, is now fully installed and running at the CERN Large Hadron Collider. In this paper the detector will be described. Some results from commissioning the detector with first single beam data from 2008 as well as cosmic ray data will be presented. Some physics expectations from the coming first year of LHC collision data will also be given.

## 1 Introduction

ATLAS is one of the two general-purpose detectors at the Large Hadron Collider (LHC), a proton collider designed to produce proton-proton collisions at a centre-of-mass energy of 14 TeV. The LHC started successfully circulating proton beams at the injection energy of 450 GeV per beam in September 2008. However, an incident involving a superconducting bus bar between two dipole magnets led to a shut-down period of more than one year for repair and consolidation work. At the time of writing these proceedings (January 2010) the LHC has successfully restarted, and proton-proton collisions at the world energy record of 2.36 TeV were already achieved at the end of 2009 before the short winter stop. During 2010 the plans are to restart in mid February going as fast as possible to a centre-of-mass energy of 7 TeV, possibly increasing towards 10 TeV during the year. An integrated luminosity of a few hundred  $\text{pb}^{-1}$  of collision data is expected to be delivered.

The ATLAS Collaboration comprises around 2800 physicists from 169 institutions in 37 countries (at the time of writing the number of institutions has increased to 172). After close to 20 years of construction and installation work the ATLAS detector was installed and working well for the first beam in 2008. Since then it has been further improved and commissioned with cosmic ray data. This paper will describe the status of the detector, some results obtained with single beam and cosmic ray data from 2008 as well as some expectations of first physics with high energy collision data.

## 2 The ATLAS Detector

The ATLAS detector [1, 2] is designed to have excellent tracking, calorimetry and muon detection over the full energy range available at the LHC. A schematic view of the detector, where the different parts are labelled, can be found in Figure 1. The huge detector has a cylindrical shape of 44 m length and 25 m diameter. It weighs around 7000 tons.

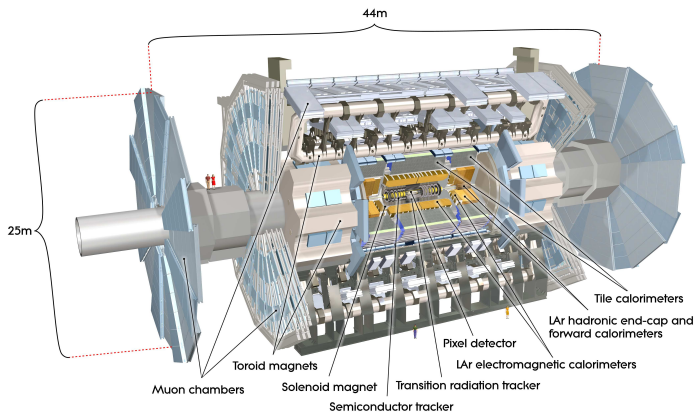


Figure 1: Schematic view of the ATLAS detector.

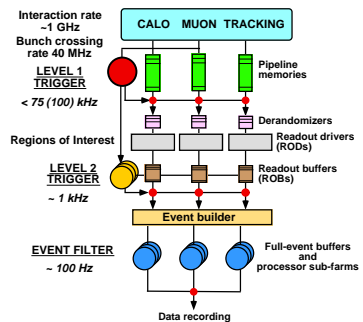


Figure 2: Schematic view of the ATLAS trigger and DAQ systems.

The innermost detector part is the Inner Detector (ID). It consists of three subdetectors, the pixel detector, the Semi-Conductor Tracker (SCT) and the Transition Radiation Tracker (TRT).

The ID covers a pseudorapidity region of  $|\eta| < 2.5$ . It is enclosed by a solenoid magnet providing an axial field of 2 T. The pixel detector has three layers of pixels both in the barrel and the endcap regions and has 80 million channels. The SCT consists of four double layers of silicon strips in the barrel region and nine in the endcap. It has around 6 M channels. The TRT, which is made of straw tube layers interleaved with transition radiation material, provides  $e - \pi$  separation in the energy range of  $0.5 < E < 150$  GeV. The TRT has  $3.5 \times 10^5$  channels. The momentum resolution provided by the combined inner detector is  $\sigma(p_T)/p_T \simeq 3.4 \times 10^{-4} p_T/\text{GeV} \oplus 0.015$ .

The calorimeter system is situated outside the solenoid magnet. The calorimeters have a coverage up to  $|\eta| = 5$ . The electromagnetic (EM) calorimeter uses a sampling technique with accordion shaped lead plates as absorbers and Liquid Argon (LAr) as sensitive material both in the barrel and in the endcap regions ( $|\eta| < 3.2$ ). The EM energy in the forward region is measured by the first layer of the forward calorimeter (LAr/copper). The hadron calorimeter is a sampling iron - scintillating tiles calorimeter (Tilecal) in the barrel region,  $|\eta| < 1.7$ . In the endcap and forward regions there are LAr calorimeters with copper/tungsten as absorber material respectively. The relative energy resolution of the electromagnetic calorimeter is  $\sim 10\% \sqrt{E}$ . In the hadron barrel region the relative jet resolution is  $\sim 50\% / \sqrt{E} \oplus 0.03$ .

The outermost system is the huge muon spectrometer. Two different technologies are used for the precision chambers. For most regions Monitored Drift Tubes (MDT) are used. In the endcap inner region Cathode Strip Chambers (CSC) are used since they are able to cope with higher background rates. Also the trigger chambers are made with two different technologies. Resistive Plate Chambers (RPC) are used in the barrel and Thin Gap Chambers (TGC) in the endcap regions. The barrel muon detectors are surrounded by eight huge air-filled toroid coils providing a bending field of 1.5 – 5.5 Tm in the central region ( $|\eta| < 1.4$ ). In each endcap there is also a toroidal magnet system with eight coils in a common cryostat providing approximately 1 – 7.5 Tm ( $1.6 < |\eta| < 2.7$ ). The standalone muon momentum resolution is designed to be  $\Delta p_T/p_T < 10\%$  up to  $E_\mu \sim 1$  TeV.

ATLAS has a three-level trigger system successively reducing the rate from the bunch crossing rate of 40 MHz to the rate of events being written to tape of around 200 Hz. The trigger and data acquisition (DAQ) system is schematically shown in Figure 2. The level 1 trigger is implemented in hardware based on the calorimeter and muon systems. The high level triggers (level 2 and the event filter) use computer farms with around 500 and 1800 multi-core processors respectively, analysing full granularity data. At level 2 only full readout granularity data from so called "regions of interest" are analysed. Only 35% of the high level trigger hardware is currently installed. This is completely adequate for the first year of data taking.

To cope with the massive need for computing infrastructure a world-wide computing network, the World-wide LHC Computing Grid, has been built. ATLAS has around 70 computing sites distributed over the world. The operational challenges (e.g.  $\sim 50$  PByte of data to be moved across the world every year,  $10^9$  raw events per year to be processed and reprocessed) and the complex Computing Model have been stress-tested and refined over the last years through functional tests and data challenges of increasing functionality, size and realism.

### 3 Commissioning with single beam data

During the short single beam run in September 2008 ATLAS collected data from beam halo events and so called beam-splash events, which were produced when bunches of around  $2 \times 10^9$  protons at 450 GeV were stopped by closed collimators upstream of the experiment. An example of such a beam-splash event is shown in Figure 3. The whole detector was lit up, mainly by the muons resulting from the "splash", depositing around 100 TeV in the detector. The first beams on September 10-12 were very useful to synchronize the various sub-detectors, in particular to start timing-in the trigger. The timing of the various components (sub-detectors, trigger system) was synchronized with respect to the so called ATLAS beam pick-ups (BPTX) reference. An adjustment to within one bunch crossing, 25 ns, was achieved in these two days. The detection of the single beam data showed that ATLAS was ready for data taking in September 2008.

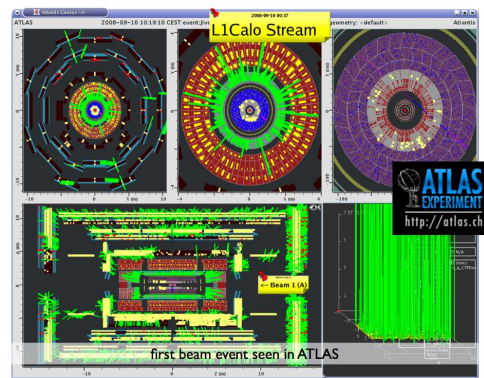


Figure 3: First beam in ATLAS.

### 4 Commissioning with cosmic ray data

After the LHC incident on 19 September 2008 ATLAS has made good use of the extra time to commission and validate all aspects of the detector. Global cosmic runs with the full detector operational were performed in the autumn of 2008. Around 500 M events were collected in August – October 2008 producing around 1.2 PByte of raw data. Over 200 M events were collected with the full detector being read out. Data were taken both with and without the magnetic field being switched on. The cosmic ray data were very useful to debug the experiment,

to study and validate the calibration and alignment and to gain in situ experience with the global detector operation. The detector was opened in October 2008 for maintenance, consolidation and a few repairs. In the beginning of June 2009 the detector was closed again and global cosmics runs were restarted at the end of June. In this section some results from the cosmic runs in the autumn of 2008 will be discussed.

#### 4.1 The inner detector

To achieve the precise measurements of tracks and knowledge of the absolute momentum scale to  $\ll 0.1\%$ , needed e.g. for a measurement of the W mass, a precise alignment of the detectors is required. Alignment of the inner detector was studied with the cosmic ray data. An example is given in Figure 4, where the pixel residual distribution is shown. The residual is defined as the difference between the measured hit position and the expected hit position from the track extrapolation. The broadest distribution corresponds to the residuals with nominal geometry. The distribution with the filled circles corresponds to the residuals after alignment with cosmic rays and the most narrow distribution, with the open circles, to a Monte Carlo (MC) simulation with perfect geometry. Both for the pixel and for the SCT detectors a precision of around  $20 \mu\text{m}$  was achieved close to the ultimate goal of  $5 - 10 \mu\text{m}$ .

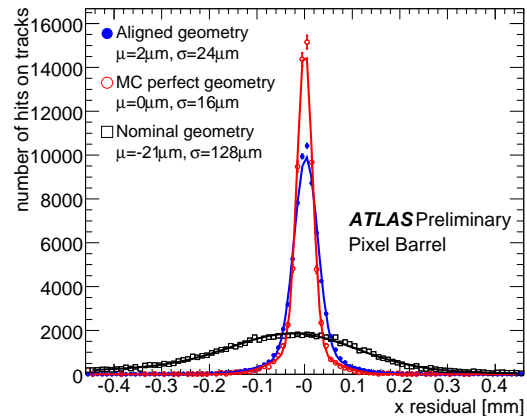


Figure 4: Pixel detector alignment with cosmic ray data compared to the MC expectation.

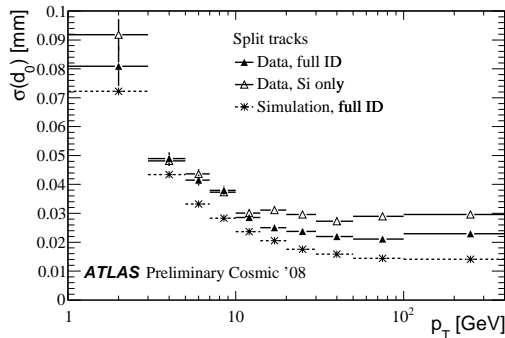


Figure 5: Impact parameter resolution plotted versus  $p_T$

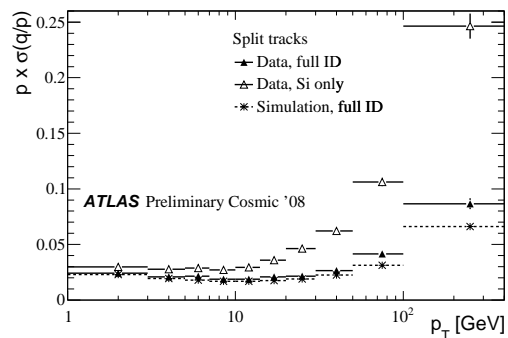


Figure 6: Momentum resolution plotted versus  $p_T$ .

Cosmic ray tracks crossing the whole inner detector were used to measure the track parameter resolution. The tracks were split in the center and refitted separately. By comparing the parameters of the two collision-like tracks originating from the same cosmic muon the res-

olution could be measured. In Figure 5 the transverse impact parameter resolution is plotted as a function of  $p_T$ . The plot shows comparisons of tracks using the full ID (closed triangles), only the silicon sub-detectors (open triangles) and tracks from cosmic simulation using the full ID (stars). In the low  $p_T$  region, the resolution is dominated by multiple scattering effects. Taking into account the TRT information improves the resolution. In Figure 6 the corresponding plot for the relative momentum resolution is shown. The relative momentum resolution increases with higher  $p_T$  due to stiffer tracks and a more difficult measurement of the sagitta. Including information from the TRT extends the lever arm and helps improve the resolution. The obtained resolution is already quite close to the ideal MC simulation.

Studies of the transition radiation in the TRT were also performed. The transition radiation intensity is proportional to the particle  $\gamma$ -factor. In Figure 7 the turn-on of the transition radiation at values of the  $\gamma$ -factor of around 1000 is shown. For muons this corresponds to a momentum of around 100 GeV. On the y-axis the probability of a high-threshold hit, which is an indicator of transition radiation, is given. The data points are shown for cosmic muons separately for both charges and are compared to the results obtained in the ATLAS Combined Test Beam in 2004 (black thin line). The turn-on of the transition radiation is nicely seen and the identical behaviour of the detector to cosmic

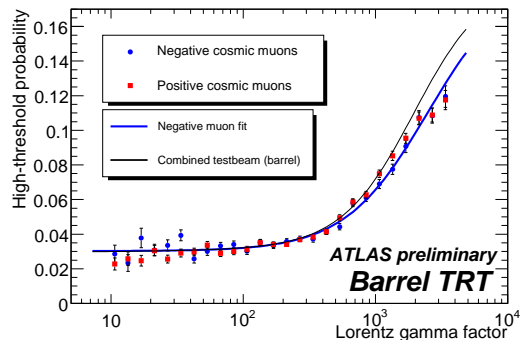


Figure 7: Turn-on of transition radiation in the TRT barrel.

tracks and data recorded at the test beam demonstrates that the TRT is working properly.

## 4.2 The muon spectrometer

A very good momentum resolution for muons is important for the possibility to e.g. discover new heavy resonances decaying to a muon pair as a "narrow" peak. The muon  $p_T$  resolution varies from 5% at 10 GeV up to about 10% at 1 TeV. The latter can be achieved provided that the muon chambers will be aligned to about  $30 \mu\text{m}$ . Cosmic ray data taken without the magnetic field were used for alignment studies. In Figure 8 are shown the measured residuals for cosmic data taken without magnetic field. For a properly aligned muon chamber tower the mean value of the residual is expected to be within the required  $30 \mu\text{m}$ . The three plots show the residual distributions for tracks going through a particular muon chamber for three different geometries: the top distribution is obtained using nominal geometry, the middle one using the geometry based on the optical alignment system and the bottom one is obtained after alignment with straight tracks. The improvement between the steps is clearly seen and the result is very promising.

Studies have also been made checking the correlation between track measurements in the inner detector and the muon spectrometer. In Figure 9 the difference between the measurements of the momentum of a track in the lower part of the detector using the ID and using the muon spectrometer is shown. The peak value of around 3 GeV/c corresponds to the expected energy loss of the muon in the calorimeter. The measurements agree well with a Monte Carlo simulation.

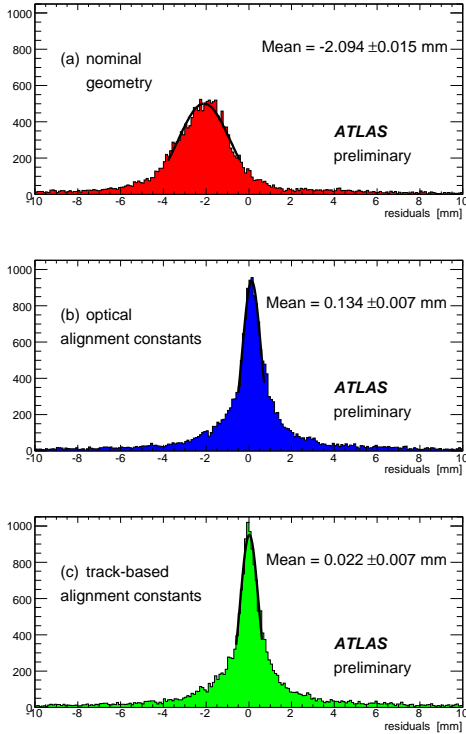


Figure 8: Alignment of the Muon Spectrometer.

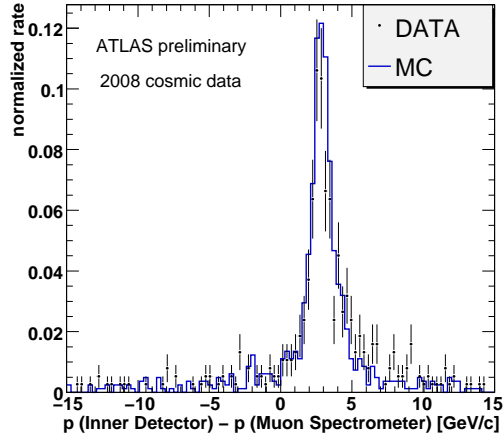


Figure 9: The difference of the momentum measured in the ID and the muon spectrometer for tracks in the bottom part of the detector.

### 4.3 The calorimeter system

Many studies of calorimeter performance were made with cosmic ray data. Here will be shown examples of how noise studies and studies of cosmic ray data can be used to study backgrounds of fake missing energy.

The ATLAS LAr calorimeter system has recorded several millions of cosmic ray and random trigger events. Detailed understanding and improvement of the signal reconstruction has made it possible to study the performance on these events of higher level quantities such as the missing transverse energy,  $E_T^{miss}$ . The performance of the standard calorimeter  $E_T^{miss}$  algorithms, as planned to be used for the analysis of the collision data, is shown in Figure 10. The missing transverse energies in the LAr calorimeter are reconstructed using all cells above a noise threshold of two standard deviations ( $|E| > 2 \times \sigma_{noise}$ ). The width of the energy distribution in each cell,  $\sigma_{noise}$ , has been estimated on a cell by cell basis for all LAr sub-detectors as the RMS of the energy distribution in a calibration run. The analysis is performed with random and first level calorimeter (L1Calo) triggered events. Inclusive distributions of  $E_T^{miss}$  for both types of events are shown together with a simple MC simulation, which is based on randomisation of the cell energy with a gaussian noise. L1Calo events, triggered by hard bremsstrahlung photons from muons, are mainly originating from the Tilecal. Consequently the  $E_T^{miss}$  distribution in

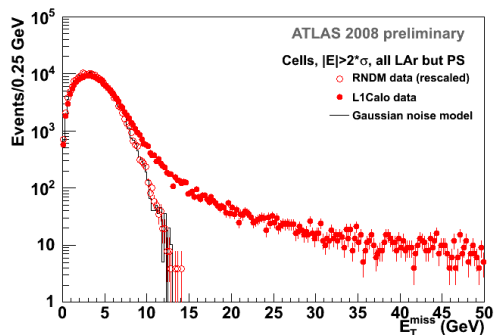


Figure 10: Distribution of the missing energy in events triggered by the calorimeter. The noise from random events is described in the text.

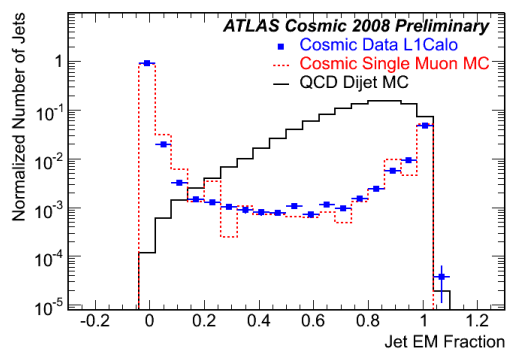


Figure 11: The distributions of the EM fraction of jets for cosmic data and QCD dijet MC.

most cases corresponds to the random event distribution. The high energy tail corresponds to real energy deposit in one of the LAr sub-detectors.

Jets and large missing transverse energy can originate from high energy cosmic muons passing the ATLAS calorimeter. The aim of the study shown in Figure 11 is to investigate the performance of cleaning cuts against cosmic rays. The jet EM fraction is the ratio of the energy deposited in the EM calorimeter and the whole calorimeter. The jet EM fraction from the cosmic L1Calo data stream, a cosmic MC simulation, and QCD di-jet MC samples simulating proton-proton collisions are shown. Only jets with  $E_T > 20$  GeV are included. The distributions were normalized by the total number of jets. The most likely value for the EM fraction is 0 or 1 for fake jets from cosmics, since the high energy deposit from photons originating from high energetic muons will localize either in the EM or the hadronic calorimeter. The QCD jets have a broad distribution of the EM fraction peaking around 0.8. A good separation between real QCD jets and fake jets from cosmics is observed. Selection cuts around 0 and 1 can remove most of the fake jets while keeping most of the jets produced in proton-proton collisions.

#### 4.4 First electrons seen in ATLAS

A study has been made to identify electrons in cosmic ray data. The electrons are expected to be produced as  $\delta$ -rays from ionisation of cosmic muons. The analysis was performed on a sample of 3.5 million events selected by the level-two track trigger. The tracks used were required to have a loose association to an EM calorimeter cluster with a transverse energy above  $\sim 3$  GeV and after some further cuts the events were split into two categories. One sample consisted of 1229 muon bremsstrahlung candidates with only one track reconstructed in the barrel inner detector. The other sample consisted of 85 ionisation electron candidates with at least two tracks reconstructed in the barrel inner detector. In Figures 12 and 13 scatter plots are shown for the two event categories respectively, where the TRT signal, expressed as the ratio of the number of high to to the number of low threshold hits in the TRT, is plotted versus the ratio of the energy measured in the EM calorimeter and the momentum measured in the ID. The dashed lines in the figures indicate the electron signal region:  $0.8 < E/p < 2.5$  and the high to low threshold TRT hit ratio

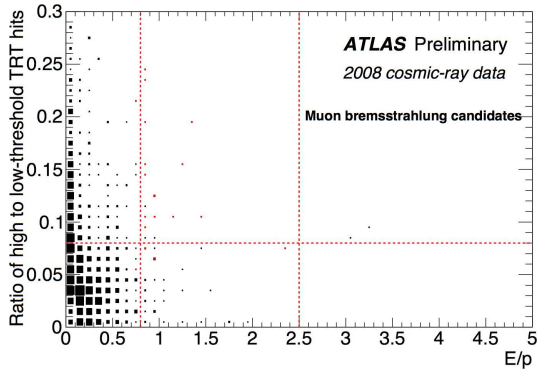


Figure 12: Ratio of high to low threshold TRT hits plotted versus  $E/p$ , where  $E$  is measured in the EM calorimeter and  $p$  in the inner detector, for bremsstrahlung candidates.

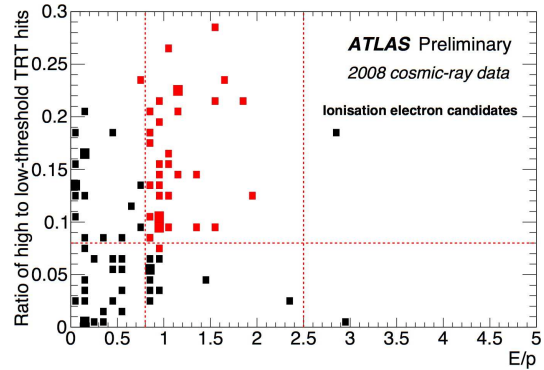


Figure 13: Ratio of high to low threshold TRT hits plotted versus  $E/p$ , where  $E$  is measured in the EM calorimeter and  $p$  in the inner detector, for ionisation electron candidates.

$> 0.08$  (indicating the detection of transition radiation produced only by relativistic particles).

Most of the events in Figure 12 have small  $E/p$  ratio and few high threshold TRT hits. Only 19 of the 1229 events satisfy the signal criteria. In contrast, in the event sample shown in Figure 13, a large fraction of events, 36 out of the total of 85, satisfy the signal criteria. These events are interpreted as high energy  $\delta$ -rays produced in the inner detector volume by the incoming cosmic muons. In Figure 14 the distribution of the energy to momentum ratio for the electron candidates of Figure 13, after applying the cut indicated on the ratio of high to low threshold TRT hits, is displayed. The background curve is estimated using both the electron candidates outside the signal region in Figure 13 and the muon bremsstrahlung candidates in Figure 12. A clear accumulation of signal events around  $E/p = 1$  is observed, as expected for electrons. Out of the 36 signal candidates, 32 have a measured negative charge, and these constitute the final sample. This is the first observation of electrons in the ATLAS detector.

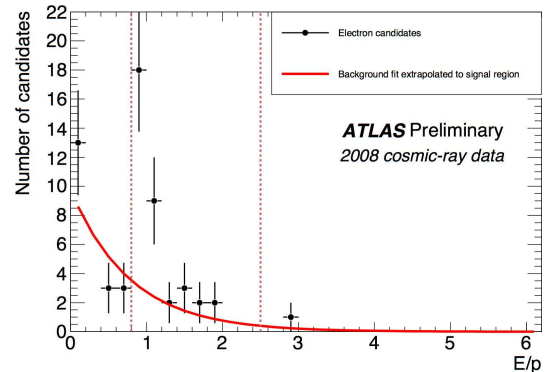


Figure 14: The distribution of the  $E/p$  ratio for the electron candidates of Figure 13 after applying the cut indicated on the ratio of high to low threshold TRT hits.

## 5 Detector status after the winter 2008-2009 shut-down

Only a few examples of commissioning results were discussed in the previous section. Also the trigger and DAQ systems as well as the computing system were successfully commissioned. For example comparisons between the trigger and the full readout gave very good results.

After the commissioning runs with cosmic rays in 2008 and the repair and consolidation work in the winter 2008-2009 shut-down the detector was efficient to the few per mille level as can be seen in Table 1. The overall data taking efficiency, calculated over dedicated 6-14 hour long simulated LHC stores, has already reached  $\sim 83\%$ . Some concerns are the long-term reliability of some components: the low-voltage power supplies of the LAr and Tile calorimeters, the LAr calorimeter readout optical links, and the inner detector cooling. Back-up solutions are being prepared for installation in future shut-down periods.

Sub-detector	Number of channels	Operational fraction(%)
Pixels	80 M	98.5
SCT	6 M	99.5
TRT	350 k	98.2
LAr EM calo	170 k	99.1
Tile calo	9800	99.5
LAr Hadronic endcap	5600	99.9
LAr Forward calo	3500	100
MDT	350 k	99.3
CSC	31 k	98.4
RPC	370 k	$\sim 95.5$ (aim $>98.5$ )
TGC	320 k	99.8

Table 1: Detector status after the winter 2008-2009 shut-down.

## 6 Examples of physics with first LHC data

When high-energy collision data will become available the commissioning and calibration of the detector in situ will be done using well-known physics samples. When the first tens of  $\text{pb}^{-1}$  are collected already a few hundred thousand  $J/\psi$  and several thousand  $\Upsilon$  decays to muon pairs will be available. Further very useful event samples will be e.g.  $Z$  decays to muon and electron pairs and  $W$  decays to jets. These samples will be used for alignment and calibration of the muon spectrometer and the ID, for the EM calorimeter calibration, for the energy/momentum scale of the full detector, for lepton trigger and reconstruction efficiency etc.

The next step before searching for discoveries is to measure Standard Model processes, e.g. production of  $Z$ ,  $W$ ,  $t\bar{t}$ , QCD jets. In Figure 15 an example of simulated top pair production is shown [3]. Events with top pairs where one top quark decays to a b-quark, a lepton and a neutrino and the other to a b-quark and two light quarks are selected. The requirements are thus to have an event with four high  $p_T$  jets, a high  $p_T$  lepton and missing transverse energy. The lepton is used for triggering and the plot shows the invariant mass of the combination of three jets with the highest  $p_T$ . The analysis is relatively simple and requires no  $b$ -tagging. The plot contains events in the muon decay channel and corresponds to an integrated luminosity of  $200 \text{ pb}^{-1}$  at a collision energy of 10 TeV. After cuts the estimated number of events in the muon decay channel is around 1600. An analysis at 7 TeV with the same integrated luminosity would have yielded around 600 events. Event samples of this size should be available during the 2010 LHC run. The expected uncertainty on the measured top cross section at  $\sqrt{s}=10$  TeV is less than 20% not including the luminosity uncertainty. The top measurement requires good understanding of most signatures essential for searching for new physics e.g. leptons, jets, missing transverse energy,  $b$ -jets. Also top will constitute an important background to most searches for new physics. When the top is measured the experiment is ready for the discovery phase.

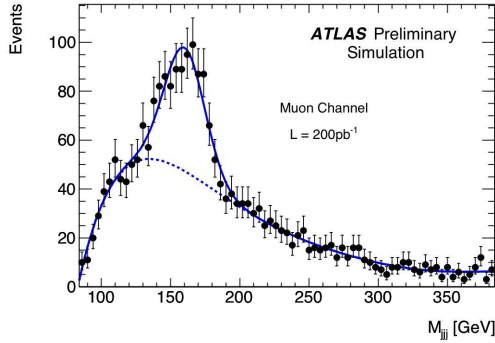


Figure 15: Invariant mass spectrum for the combination of three jets with highest  $p_T$  in events with top pairs, one top decaying leptonically in the muon channel and the other decaying hadronically.

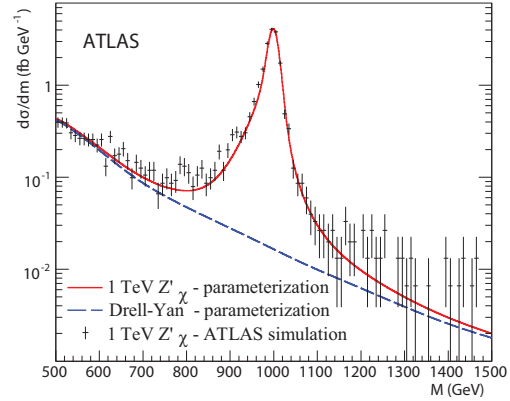


Figure 16: Mass spectrum for a  $m = 1$  TeV  $Z'_\chi \rightarrow e^+e^-$  obtained with ATLAS full simulation.

A possibility of an early physics surprise could be a narrow mass peak in the dilepton invariant mass spectrum. An example is given in Figure 16 [2]. The figure results from a simulation of  $Z'_\chi$  with a mass of 1 TeV decaying to  $e^+e^-$  pairs.  $Z'$  particles appear in many models beyond the Standard Model. This particular simulation refers to production of a sequential Standard Model-like  $Z'$ . The signal is nicely seen above a small and smooth SM background. This analysis does not require the ultimate EM calorimeter performance. The analysis is made at  $\sqrt{s} = 14$  TeV. A discovery at the level of  $5\sigma$  at this energy would require an integrated luminosity of around  $50 \text{ pb}^{-1}$ . At  $\sqrt{s} = 7$  TeV the estimated integrated luminosity to reach a sensitivity just beyond the current Tevatron limits of around 1 TeV is around  $200 \text{ pb}^{-1}$  (around  $100 \text{ pb}^{-1}$  at 10 TeV). This should be possible to achieve during the 2010 LHC run.

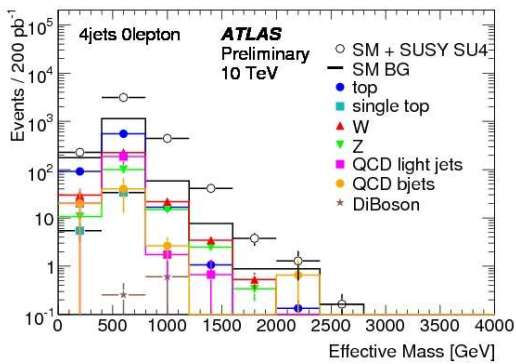


Figure 17: Effective mass distribution for the 4 jets channel with 0 leptons.

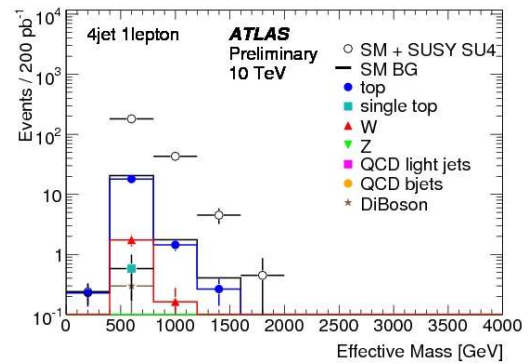


Figure 18: Effective mass distribution for the 4 jets channel with 1 lepton.

If supersymmetry (SUSY) exists with a mass scale of squarks and gluinos of around 1 TeV

it could be one of the first discoveries at the LHC. A huge production cross-section could be expected. The decay chains of the squarks or gluinos are expected to give rise to spectacular final states with many jets, leptons, and, in particular for R-parity conserving models, missing transverse energy. Of particular interest is of course that the stable lightest SUSY particle, the neutralino, is a dark matter candidate. Figures 17, 18 and 19 are based on a simulation study of inclusive SUSY searches in the minimal Supergravity model made at a centre-of-mass energy of 10 TeV assuming an integrated luminosity of  $200 \text{ pb}^{-1}$  [4]. Figures 17 and 18 show examples of distributions of the effective mass for signal and background events. The effective mass is the scalar sum of the transverse momenta of the main objects like leading jets, leptons, missing  $E_T$ . It is one of the variables used for sample defining cuts. These figures are

produced for squark and gluino masses around 410 GeV. Figure 17 shows the effective mass distribution for the 4 jets channel with zero leptons and Figure 18 shows the distribution for the channel including one lepton. It can be seen from the figures that the jets and missing  $E_T$  channel gives highest reach, whereas the channel including one lepton in the final state is more robust against background. In Figure 19 the  $5\sigma$  discovery reach as a function of  $m_0$  and  $m_{1/2}$  for channels with 0, 1 and 2 leptons is shown. The particular model used here is mSUGRA with  $\tan\beta = 10$ . The full, green line corresponds to the channel with 4 jets and no leptons, and the dashed-dotted, black line to the channel with 4 jets and 1 lepton. The discovery reach is squark and gluino masses of around 750 GeV. Going to  $\sqrt{s} = 7 \text{ TeV}$ , the discovery reach for  $200 \text{ pb}^{-1}$  is still expected to be beyond the expected Tevatron reach of around 400 GeV. It will however take some time to understand the tricky backgrounds, in particular fake missing transverse energy. The ultimate discovery reach at LHC is expected at masses around 3 TeV.

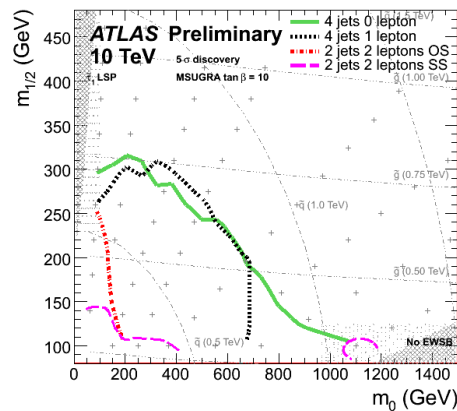


Figure 19:  $5\sigma$  discovery reach as a function of  $m_0$  and  $m_{1/2}$  for the mSUGRA model with  $\tan\beta = 10$ .

## 7 Conclusions

The ATLAS experiment is in excellent shape. The fraction of non-working channels is on the few per mille level. Analysis of  $\sim 600 \text{ M}$  cosmic events, as well as single beam data in Sept 2008, shows better detector performance than expected at this stage. Software and computing have proved to be able to cope with simulation, analysis and world-wide distribution of massive amounts of data. After 20 years of efforts building all aspects of the experiment ATLAS is ready for LHC collisions data.

At the time of writing, January 2010, ATLAS has in fact taken around 1 M collision events provided by LHC late 2009. The preliminary analysis shows that all aspects of ATLAS work very well and that ATLAS is ready for the next phase of high energy collisions.

## Acknowledgements

We are greatly indebted to all CERN's departments and to the LHC project for their immense efforts not only in building the LHC, but also for their direct contributions to the construction and installation of the ATLAS detector and its infrastructure. We acknowledge equally warmly all our technical colleagues in the collaborating Institutions without whom the ATLAS detector could not have been built. Furthermore we are grateful to all the funding agencies which supported generously the construction and the commissioning of the ATLAS detector and also provided the computing infrastructure.

The ATLAS detector design and construction has taken about fifteen years, and our thoughts are with all our colleagues who sadly could not see its final realisation.

We acknowledge the support of ANPCyT, Argentina; Yerevan Physics Institute, Armenia; ARC and DEST, Australia; Bundesministerium für Wissenschaft und Forschung, Austria; National Academy of Sciences of Azerbaijan; State Committee on Science & Technologies of the Republic of Belarus; CNPq and FINEP, Brazil; NSERC, NRC, and CFI, Canada; CERN; NSFC, China; Ministry of Education, Youth and Sports of the Czech Republic, Ministry of Industry and Trade of the Czech Republic, and Committee for Collaboration of the Czech Republic with CERN; Danish Natural Science Research Council and the Lundbeck Foundation; European Commission, through the ARTEMIS Research Training Network; IN2P3-CNRS and Dapnia-CEA, France; Georgian Academy of Sciences; BMBF, DESY, DFG and MPG, Germany; Ministry of Education and Religion, through the EPEAEK program PYTHAGORAS II and GSRT, Greece; ISF, MINERVA, GIF, DIP, and Benozio Center, Israel; INFN, Italy; MEXT, Japan; CNRST, Morocco; FOM and NWO, Netherlands; The Research Council of Norway; Ministry of Science and Higher Education, Poland; GRICES and FCT, Portugal; Ministry of Education and Research, Romania; Ministry of Education and Science of the Russian Federation, Russian Federal Agency of Science and Innovations, and Russian Federal Agency of Atomic Energy; JINR; Ministry of Science, Serbia; Department of International Science and Technology Cooperation, Ministry of Education of the Slovak Republic; Slovenian Research Agency, Ministry of Higher Education, Science and Technology, Slovenia; Ministerio de Educación y Ciencia, Spain; The Swedish Research Council, The Knut and Alice Wallenberg Foundation, Sweden; State Secretariat for Education and Science, Swiss National Science Foundation, and Cantons of Bern and Geneva, Switzerland; National Science Council, Taiwan; TAEK, Turkey; The Science and Technology Facilities Council and The Leverhulme Trust, United Kingdom; DOE and NSF, United States of America.

## References

- [1] The ATLAS Collaboration, G. Aad *et al.*, *The ATLAS Experiment at the CERN Large Hadron Collider*, JINST **3** S08003 (2008).
- [2] The ATLAS Collaboration, G. Aad *et al.*, *Expected Performance of the ATLAS Experiment, Detector, Trigger and Physics*, CERN-OPEN-2008-020 (2008).
- [3] The ATLAS Collaboration, *Prospects for the Top Pair Production Cross-section at  $\sqrt{s} = 10$  TeV in the Single Lepton Channel in ATLAS*, ATL-PHYS-PUB-2009-087 (2009)
- [4] The ATLAS Collaboration, *Prospects for SUSY and UED discovery based on inclusive searches at a 10 TeV centre-of-mass energy with the ATLAS detector*, ATL-PHYS-PUB-2009-084 (2009)

## Discussion

**Dmitri Denisov (FNAL):** What are major factors defining 20% expected data taking inefficiency during initial ATLAS operation?

**Answer:** The factors affecting the initial data taking efficiency for cosmic muons are being evaluated in detail at the moment. I don't know of any single large factors.

**Vera Lüth (SLAC):** At present, how long does it take to produce a typical high-pT event on a multi-core CPU unit (simulation)?

**Answer:** I don't have this number at the top of my head. It is not a limiting factor in our analysis. (Afterwards I have found out that the time for a full simulation is of the order of 2000 kSI2Kseconds depending on the type of event.)

**Eckhard Elsen (DESY):** Is the noise contributing to the ET-miss measurement already at the experimentally expected limit? What is the contribution from coherent noise etc...?

**Answer:** We are already in a rather good shape describing the noise. We continue to investigate the issue, in particular the tails of the noise distributions.

**Vali Huseynov (Nakhchivan State University):** One of the main mission of the ATLAS experiment is to test the existence of additional dimensions. How many additional dimensions do you expect from this experiment?

**Answer:** This is of course hard to tell. We certainly have strategies to investigate different models including extra dimensions. I mentioned one example. A spin analysis of a potential discovery of a narrow mass peak in the di-lepton invariant mass spectrum might disentangle a Z with spin one from a graviton resonance of spin two, the latter being a manifestation of extra dimensions.

**Ahmed Ali (DESY):** This is about the discovery potential of the SM Higgs boson at the LHC. Since the data taking will take place in the first stage at 7 to 10 TeV and the luminosity of the LHC is also scaled down in this phase, how long will it take the experiment at the LHC to be competitive with the ongoing experiments at the TeVatron in the SM Higgs search?

**Answer:** Considering that at 7 TeV the cross section for a Higgs boson, just above the mass limit set by LEP, is expected to be around 30cross section at 14 TeV, it will most likely take a couple of years until LHC is fully competitive.